Neurobiology of Disease

Hippocampal Neurogenesis and Neural Circuit Formation in a Cuprizone-Induced Multiple Sclerosis Mouse Model

Hai Zhang,[1] Yeonghwan Kim,[2] Eun Jeoung Ro,[1] Cindy Ho,[1] Daehoon Lee,[1] Bruce D. Trapp,[1] and Hoonkyo Suh[1]
Departments of [1]Neurosciences, and [2]Cancer Biology, Lerner Research Institute, Cleveland Clinic, Cleveland, Ohio 44195

Cognitive impairments are key features in multiple sclerosis (MS), a progressive disorder characterized by neuroinflammation-induced demyelination in the central nervous system. To understand the neural substrates that link demyelination to cognitive deficits in MS, we investigated hippocampal neurogenesis and synaptic connectivity of adult-born neurons, which play an essential role in cognitive function. The administration and withdrawal of the combination of cuprizone and rapamycin (Cup/Rap) in C57BL/6J male mice efficiently demyelinated and remyelinated the hippocampus, respectively. In the demyelinated hippocampus, neurogenesis was nearly absent in the dentate gyrus, which was due to inhibited proliferation of neural stem cells (NSCs). Specifically, radial glia-like type 1 NSCs were shifted from a proliferative state to a mitotically-quiescent state in the demyelinated hippocampus. In addition, dendritic spine densities of adult-born neurons were significantly decreased, indicating a reduction in synaptic connections between hippocampal newborn neurons and excitatory input neurons. Concomitant with hippocampal remyelination induced by withdrawal of Cup/Rap, proliferation of type 1 NSCs and dendritic spine densities of adult-born neurons reverted to normal in the hippocampus. Our study shows that proliferation of hippocampal NSCs and synaptic connectivity of adult-born neurons are inversely correlated with the level of demyelination, providing critical insight into hippocampal neurogenesis as a potential therapeutic target to treat cognitive deficits associated with MS.

Key words: **hippocampus; neurogenesis; synaptic connectivity; cuprizone; multiple sclerosis**

Significance Statement

To identify the neural substrates that mediate cognitive dysfunctions associated with a majority of MS patients, we investigated hippocampal neurogenesis and structural development of adult-born neurons using a Cup/Rap model, which recapitulates the hippocampal demyelination that occurs in MS patients. A shift of NSCs from a proliferatively-active state to mitotically-quiescent state dramatically decreased neurogenesis in the demyelinated hippocampus. Formation of dendritic spines on newborn neurons was also impaired following demyelination. Interestingly, the altered neurogenesis and synaptic connectivity of newborn neurons were reversed to normal levels during remyelination. Thus, our study revealed reversible genesis and synaptic connectivity of adult-born neurons between the demyelinated and remyelinated hippocampus, suggesting hippocampal neurogenesis as a potential target to normalize cognitive impairments in MS patients.

Introduction

Multiple sclerosis (MS) is an inflammatory-mediated demyelinating disease of the central nervous system (CNS) that afflicts more than 1 million individuals in the United States (Noseworthy et al., 2000; Wallin et al., 2019). MS is a progressive and chronic neurological disease that often begins in the third or fourth decade of life and eventually reduces lifespan by 7–8 years. Although MS was historically considered to be a white-matter disease, it is now well established that cortical and deep gray-matter demyelination are prominent features of MS (Gilmore et al., 2009; Trapp et al., 2018).

MS is characterized by motor, sensory, and cognitive impairments. In particular, cognitive dysfunction occurs in >50% of MS patients and negatively impacts memory, learning, and information processing speed (Chiaravalloti and DeLuca, 2008). Brain imaging studies of living MS patients implicate hippocampal atrophy and hippocampal demyelination as contributors to the cognitive decline (Longoni et al., 2015; Preziosa et al., 2016).

Received April 16, 2019; revised Oct. 16, 2019; accepted Nov. 4, 2019.

Author contributions: B.D.T. and H.S. designed research; H.Z., Y.K., E.J.R., C.H., and D.L. performed research; H.Z., Y.K., E.J.R., C.H., D.L., and H.S. analyzed data; H.Z., B.D.T. and H.S. wrote the paper.

This work was supported by the National Institute of Alcohol Abuse and Alcoholism (R01AA022377 to H.S.), the Hartwell Foundation (to H.S.), and NIH (R35 NS099588 NINDS to B.D.T.). We thank Dr. Christopher L. Nelson for editorial support, and Drs. Ranjan Dutta and Jessica Williams for productive discussions.

The authors declare no competing financial interests.

Correspondence should be addressed to Hoonkyo Suh at Suhh2@ccf.org.

https://doi.org/10.1523/JNEUROSCI.0866-19.2019

Postmortem studies of hippocampi from chronic MS brains have reported decreases in synaptic densities and molecular changes that negatively impact learning and memory (Papadopoulos et al., 2009; Dutta et al., 2011). However, because fatalities are rare during early stages of MS, little is known about the acute effects of hippocampal demyelination on cognitive dysfunctions in MS patients.

Reliable rodent models have been developed to study acute changes in the demyelinated hippocampus (Dutta et al., 2013; Sachs et al., 2014; Bai et al., 2016). The most commonly described rodent model of hippocampal demyelination involves feeding mice a diet containing cuprizone, which is a copper-chelating agent that kills oligodendrocytes. The combination of a cuprizone diet and daily intraperitoneal injections of rapamycin (Cup/Rap) has also been used to ensure more complete and consistent demyelination because rapamycin significantly lowers spontaneous remyelination associated with cuprizone treatment (Sachs et al., 2014; Bai et al., 2016). Indeed, 6–12 weeks of Cup/Rap treatment demyelinates >90% of the mouse hippocampus, and these mice have deficits in learning and memory function as measured by the Morris water maze test (Dutta et al., 2013). Replacing cuprizone chow with standard chow initiates remyelination by 6 weeks, which restores >60% of hippocampal myelin as well as learning and memory (Dutta et al., 2013). This cuprizone model, therefore, provides a useful platform to study hippocampal demyelination and remyelination.

In this study, using a Cup/Rap-induced MS model (Bai et al., 2016), we investigated hippocampal neurogenesis in the acutely demyelinated and remyelinated hippocampus. Hippocampal neurogenesis is a life-long process in which neural stem cells (NSCs) continuously generate new neurons referred as to dentate granule cells (DGCs; Gage, 2002; Suh et al., 2007). Because neuronal development and circuit integration of adult-born DGCs play an essential role in cognitive function, structural and functional changes in newborn DGCs can serve as surrogates representing cognitive function and dysfunction associated with demyelination and remyelination. Our study revealed that hippocampal neurogenesis, as well as structural development and synaptic connectivity of newborn DGCs, were severely inhibited in Cup/Rap mice. Interestingly, altered neurogenesis and synaptic connectivity of newborn DGCs that had occurred in the demyelinated hippocampus were reversed concomitant with hippocampal remyelination induced by withdrawal of Cup/Rap. This indicates that the NSC reservoir was preserved as quiescent NSCs in Cup/Rap mice, and that these mitotically-dormant NSCs were reactivated to proliferate in the remyelinated hippocampus. This study supports the concept that hippocampal neurogenesis and development of newborn DGCs are inversely correlated with the level of demyelination, providing valuable insight into hippocampal neurogenesis as a potential target to normalize cognitive impairments in MS patients.

Materials and Methods

Animals. Eight-week-old C57BL/6J male mice were purchased from The Jackson Laboratory and used in all experiments because male mice show more consistent demyelination and remyelination in response to cuprizone, whereas demyelination in female mice has been shown to be more resistant to cuprizone treatment (Taylor et al., 2009) and more variable due to the estrous cycle (Acs et al., 2009). All experimental protocols were approved by the Institutional Animal Care and Use Committee of the Cleveland Clinic Foundation.

Cuprizone treatment. The Cup/Rap treatment procedure was described in detail in a previous publication (Bai et al., 2016). Briefly, mice were fed a chow diet containing 0.3% cuprizone (Sigma-Aldrich, C9012) for 6 weeks to induce demyelination. During this time, mice were injected once daily with 10 mg/kg rapamycin intraperitoneally. Control groups included an age-matched group (AM) and a rapamycin-treated group (Rap). In some experiments, to separate the potential effects of rapamycin from cuprizone, four mouse groups were used: cuprizone only (Cup), rapamycin only (Rap), Cup/Rap, and AM. At the end of the 3 or 6 week treatment period, mice were either killed to evaluate the effects of demyelination, or switched to normal chow for an additional 6 weeks to study the effects of remyelination.

Retrovirus injection. To label hippocampal newborn neurons, mice were anesthetized with 100 mg/kg ketamine plus 10 mg/kg xylazine, and a GFP-expressing retrovirus (RV-CAG-GFP, $5\sim8 \times 10^9$ CFU/ml) was injected bilaterally into the hippocampus before the onset of Cup treatment (Golub et al., 2015). The following coordinates relative to bregma were used: anterior to posterior (AP): −2.5 mm, medial to lateral (ML): ±2.65 mm, dorsal to ventral (DV): −3.4 mm. One microliter of virus was injected into each site through a Hamilton syringe with a 33-gauge needle. The injection speed was 0.1 μl/min. The needle was retained in place for 5 min before retraction. Mice were allowed to recover for 1 week after surgery and then were fed with the cuprizone diet.

Sample collecting. Mice were injected (i.p.) with three doses of 100 mg/kg BrdU (5-bromo-2′-deoxyuridine; Sigma-Aldrich, B5002) or CldU (5-chloro-2′-deoxyuridinem; Sigma-Aldirch, C6891) at 2 h intervals at the end of 3 or 6 weeks of demyelination or 6 weeks of remyelination. Two hours after the final injection, mice were deeply anesthetized with ketamine/xylazine and perfused with 4% paraformaldehyde (PFA) in 0.1 M phosphate buffer (PB). Brains were dissected and further fixed in 4% PFA for 24 h, then transferred into 30% sucrose solution until submerged. Brains were then frozen on dry ice and cut into coronal sections (40 μm thick) on a Leica SM2010 sliding microtome. Sections were placed into anti-freezing solution containing 30% glycerol, 20% ethyl glycol, and 50% PB and were stored at −20°C until use.

Immunostaining of free-floating sections. The following antibodies were used in this study: myelin binding protein (MBP; DAKO, A0623; rabbit, 1:250); proteolipid protein (PLP; rat, 1:100; Bai et al., 2016); BrdU (Accurate, QTB0030; rat, 1:500); BrdU (BD Science, 347580; mouse, 1:500); MCM2 (Santa Cruz Biotechnology, sc-9839; goat, 1:200); Ki67 (Cell Signaling Technology, 9129; rabbit, 1:500); doublecortin (DCX; Santa Cruz Biotechnology, sc-8066; goat, 1:500); SOX2 (Millipore Bioscience Research Reagents, AB5770; rabbit, 1:500); NG2 (Millipore, AB5320; rabbit, 1:400); CC-1 (Millipore, OP80; mouse, 1:200); Iba1 (Wako, 019-19741; rabbit, 1:1000); and GFAP (rabbit; Dako, Z0344; 1:1000; guinea pig, Advanced Immuno, 1:1000). Secondary antibodies (AF488/Cy3/AF647-donkey anti-rabbit, AF488-donkey anti-goat, Cy3-donkey anti-mouse, Cy3-donkey anti-rat, Cy3-donkey anti-guinea pig) were purchased from Jackson ImmunoResearch. Every 6th or 12th section containing the hippocampus was selected for immunostaining. For immunofluorescent staining, sections were rinsed three times in tris-buffered saline (TBS) containing 0.25% Triton X-100 (TBST) for 15 min each. For MCM2 staining, an additional antigen retrieval step (10 mM citric acid, 100°C, 10 min) was performed before blocking. For BrdU and CldU staining, sections were treated with 2 M HCl for 30 min at 56°C, neutralized with 0.1 M boric acid for 10 min, and then blocked. Sections were blocked in 3% donkey serum/TBST for 1 h at room temperature (RT). Sections were then incubated in primary antibody for either 3 d (MBP, PLP, NG2, CC-1) or overnight (all others) at 4°C. After washing three times in TBST for 15 min each, sections were incubated in secondary antibody for 2 h at RT. Sections were washed in TBST, counter-stained with DAPI (Sigma-Aldrich, D9542), and mounted. For PLP staining, 3,3′-diaminobenzidine (Vector Laboratories, SK-4100) was used as chromogen, and sections were dehydrated with ethanol and cleaned with xylenes before mounting.

Quantification of immunostaining. Quantification was performed in a blinded fashion. For myelin status, three sections from the rostral, middle, and caudal parts (AP: −1.8, −2.5, and −3.2 mm from bregma) of the hippocampus per mouse were stained with PLP and MBP, and three sections of the subventricular zone (SVZ; AP: +1.0, +0.6, and +0.2 mm from bregma) were stained with MBP. Sections were then imaged under a 20× objective, imported into ImageJ (NIH), and the density was measured. For analysis of the cell-cycle markers BrdU, Ki67, and MCM2, the positive cell number in the subgranular zone (SGZ) of the right hemi-

sphere was counted under a 20× objective from every sixth (for BrdU) or 12th (for Ki67 and MCM2) section. The results are reported as the summation of cell number multiplied by 6 or 12 per mouse. For the analysis of DCX, three rostral, middle, and caudal sections of the hippocampus per mouse were imaged under a 20× objective for 1-μm-interval *z*-series images using a Keyence BZ-X700 fluorescence microscope (Osaka). The maximum projection images were then imported into ImageJ. The images of DCX were converted to 8-bit format and thresholded. The percentage area occupied by DCX-positive staining in the granular cell layer was calculated by averaging the value from the three sections for each mouse. For quantification of neurogenesis in the SVZ, every 12th section was stained with BrdU and DCX, and the same analysis was performed as used in the SGZ. For neural stem cell quantification, eight randomly chosen areas from four hippocampal sections of each mouse were captured under a 63× oil objective using a Leica SP5 confocal microscope. The *z*-stack depth was 20 μm. NSCs were defined as double-positive cells for SOX2 and GFAP with an inverted Y-shape. NSC number was counted for each area to obtain the average value for each mouse and presented as number per cubic millimeter. Furthermore, SOX2/GFAP/MCM2 triple-positive cells were defined as activated NSCs (Song et al., 2012), and the percentage of activated NSCs among total NSCs was calculated. For NG2-positive oligodendrocyte precursor cells (OPCs), the number in the hilus and molecular layer of dentate gyrus (Mol-DG) was manually counted for every 12th section and presented as the summation multiplied by 12 per mouse. For mature oligodendrocytes that were CC-1-positive, sections were analyzed with 1-μm-interval *z*-series images using a Keyence microscope. Three random areas of DG were selected for each section and the $CC1^+$ cell number in these areas was counted and expressed as number per square millimeter. For microglia, the number of Iba1-positive cells in the hilus and Mol-DG was manually counted for every 12th section and presented as the summation multiplied by 12. The soma size of microglia was measured with ImageJ software. To analyze glial proliferation in the non-neurogenic areas of DG (Mol-DG and hilus), every 12th section was double-stained with BrdU or CldU and a glial marker, and then the numbers of $BrdU^+$ or $CldU^+$ cells were counted and presented as the summation multiplied by 12. To calculate the proportion of glial cells in the proliferating cells, sections were counted under a 40× objective using a Leica confocal microscope. For 3 weeks of demyelination, the percentages of $Iba1^+$, $NG2^+$, or $GFAP^+$ cells among $BrdU^+$ cells were calculated. For 6 weeks of demyelination and remyelination, the percentage of $NG2^+$ cells among $BrdU^+$ or $CldU^+$ cells were calculated. The number of double-positive cells examined in each animal varied between 3 and 42, because there were few proliferating cells in the non-neurogenic areas of DG.

Dendritic analysis. Methods pertaining to studying the morphology of newborn neurons were described in detail previously (Golub et al., 2015). For morphological analysis, *z*-series images with 0.5 μm intervals were captured for GFP-expressing neurons under a 63× oil objective using a Leica confocal microscope. Maximum *z*-projection pictures were created in LAS AF software (Leica Microsystems) and imported into ImageJ software with NeuronJ plugin for measurements of dendritic length. For analysis of dendritic spine density, *z*-series images with 0.2 μm intervals were captured under a 63× oil objective with a digital zoom factor of 3. The distal, middle, and proximal segments of the dendrite were captured, respectively. The maximum *z*-projection images were opened in ImageJ software to measure the length of each segment. The number of spines on each segment was counted manually and are presented as the number of spines per micrometer.

Experimental design and statistical analysis. All experiments were performed on age-matched groups containing five to six mice per group. Every 6th or 12th section containing hippocampus was selected for staining and quantification. For cell size analysis of microglia, 8–10 cells were randomly selected for each animal; therefore, a total of 40–50 cells was measured for each group. For analysis of structure and spine density of newborn neurons, 4–6 neurons with intact dendritic branches were analyzed for each animal; therefore, a total of 22–30 neurons were analyzed for each group. All data are expressed as mean ± SEM. Data were analyzed by one-way ANOVAs using GraphPad Prism 7.0 software. Bonferroni's multiple-comparison *post hoc* test was applied to compare differences among groups. The significance level was set as $p < 0.05$.

Results

Cup/Rap reversibly induces hippocampal demyelination and remyelination

To achieve consistent and extensive demyelination, we used the combination of Cup/Rap and examined hippocampal demyelination (Sachs et al., 2014; Bai et al., 2016). AM mice and mice treated with Rap only were used as control groups. Six weeks of Cup/Rap treatment successfully demyelinated the hippocampus (Fig. 1*A–E*). The expression of PLP and MBP, proteins that are associated with myelin, was dramatically reduced in the Mol-DG as well as the hilus of the hippocampus compared with AM and Rap control mice (Fig. 1*B–E*; for PLP: $F_{(2,14)} = 50.7$, $p < 0.0001$, one-way ANOVA; for MBP: $F_{(2,14)} = 12.17$, $p = 0.0013$, one-way ANOVA). The density of $CC1^+$ mature oligodendrocytes was significantly decreased (>90%), indicating efficient ablation of mature oligodendrocytes in Cup/Rap mice compared with control mice (Fig. 1*F,G*; $F_{(2,14)} = 141.7$, $p < 0.0001$, one-way ANOVA). In addition, the number of $NG2^+$ OPCs was reduced by 25% in Cup/Rap mice (Fig. 1*H,I*; $F_{(2,14)} = 5.307$, $p = 0.0244$, one-way ANOVA). During the 6 week withdrawal period following 6 weeks of Cup/Rap treatment, spontaneous remyelination was observed. In the absence of Cup/Rap, the expression of myelin proteins such as PLP and MBP reverted to control levels (Fig. 1*B–E*; for PLP: $F_{(2,14)} = 0.5064$, $p = 0.615$, one-way ANOVA; for MBP: $F_{(2,14)} = 0.1679$, $p = 0.8475$, one-way ANOVA). Although the density of $CC1^+$ cells did not fully recover to the level of control mice, an increase in the number of $CC1^+$ mature oligodendrocytes was associated with remyelination (Fig. 1*F,G*; $F_{(2,14)} = 47.91$, $p < 0.0001$, one-way ANOVA). The number of $NG2^+$ OPCs was indistinguishable from control mice (Fig. 1*H,I*; $F_{(2,14)} = 1.351$, $p = 0.2957$, one-way ANOVA). These results show that the administration and withdrawal of Cup/Rap reliably induced demyelination and remyelination in the hippocampus, respectively.

Increased number and size of microglia in the Cup/Rap-treated hippocampus

To examine inflammation associated with demyelination, we examined the number, as well as the size, of $Iba1^+$ microglia as a surrogate marker for inflammation in Cup/Rap mice (Fig. 2*A*). To our surprise, 6 weeks of Cup/Rap treatment did not significantly change either the number or the size of $Iba1^+$ microglia in the demyelinated hippocampus compared with the AM group (Fig. 2*B*; for number: $F_{(2,15)} = 6.608$, $p = 0.0105$; for size: $F_{(2,130)} = 0.973$, $p = 0.3807$, one-way ANOVA), whereas a reduction in $Iba1^+$ cell number was observed in the Rap group (Fig. 2*B*). Both the number and size of $Iba1^+$ microglia were also indistinguishable from control mice when examined at 6 weeks after Cup/Rap withdrawal (Fig. 2*C*; for number: $F_{(2,14)} = 0.73678$, $p = 0.4992$; for size: $F_{(2,117)} = 0.2996$ $p = 0.7439$, one-way ANOVA). Next, we tested the possibility that microglia were activated during the early stages of demyelination. Indeed, at 3 weeks of Cup/Rap treatment, both the number and the size of $Iba1^+$ microglia significantly increased compared with the AM and Rap control groups (Fig. 2*D,E*; for number: $F_{(2,15)} = 13.7$, $p = 0.0006$; for size: $F_{(2,133)} = 28.21$, $p < 0.0001$, one-way ANOVA).

We next examined whether proliferation of microglia was attributable to an increase in the number of $Iba1^+$ microglia in the hippocampus of Cup/Rap mice. At 3 weeks of Cup/Rap treatment, the number of $BrdU^+$ cells was significantly increased in non-neurogenic areas such as the Mol-DG and hilus of the hip-

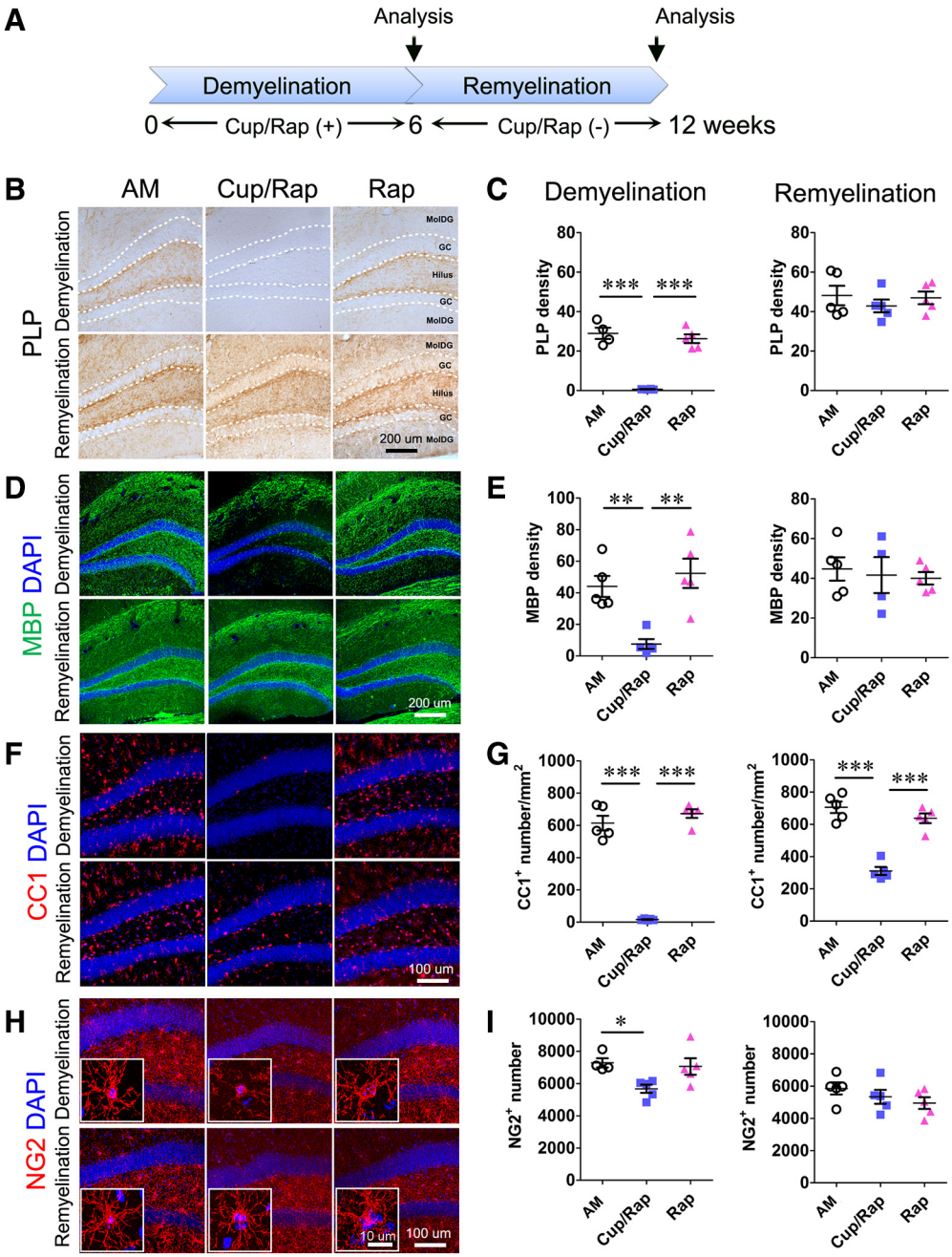

Figure 1. Expression of myelin proteins and the number of oligodendrocytes in the dentate gyrus following demyelination and remyelination. ***A***, Timeline of the experimental protocol. ***B***, Representative images showing myelin PLP staining of the dentate gyrus. ***C***, Quantification of PLP density indicates significantly reduced PLP staining in the demyelination (Cup/Rap) group. ***D***, Representative images showing MBP staining of the dentate gyrus. ***E***, Quantification of MBP density indicates significantly reduced MBP staining in the demyelination (Cup/Rap) group. ***F***, Representative images of CC1 staining showing mature oligodendrocytes. ***G***, Quantification of $CC1^+$ cell number demonstrates that mature oligodendrocytes are significantly ablated during demyelination. The number partly recovers during remyelination, but is still significantly lower than controls. ***H***, Representative images of NG2 staining showing OPCs. ***I***, Quantification of $NG2^+$ cell number demonstrates significantly decreased OPCs during demyelination, which recovers during remyelination; $n = 5$. Data are expressed as mean ± SEM and analyzed by one-way ANOVA followed by Bonferroni's *post hoc* test. $^*p < 0.05$, $^{**}p < 0.01$, $^{***}p < 0.001$.

pocampus (Fig. 3*A*,*B*; $F_{(2,15)} = 8.857$, $p = 0.0037$, one-way ANOVA). Interestingly, $Iba1^+$ microglia represented the major proliferating cell population among $BrdU^+$-dividing cells in non-neurogenic areas at 3 weeks of demyelination (Fig. 3*C*; $F_{(2,15)} = 22.55$, $p < 0.0001$, one-way ANOVA), whereas $NG2^+$ OPCs were the predominantly dividing cells in control mice (Fig. 3*C*; $F_{(2,15)} = 13.76$, $p = 0.0006$, one-way ANOVA). In both 6 weeks of Cup/Rap treatment and following 6 weeks of withdrawal of Cup/Rap, the number of dividing cells, as well as the proportions of dividing cell types, were not different from control mice (Fig. 3*B*,*D*,*E*), indicating that increased proliferation of $Iba1^+$ cells contributed to the induction of $Iba1^+$ cells at the early stage of Cup/Rap treatment (Fig. 3*D*,*E*). Proliferating $GFAP^+$ astrocytes were not detected at any of the three time points that we analyzed in either control or Cup/Rap mice (Fig. 3*C*; and data not shown).

Reversible changes in hippocampal neurogenesis during treatment and withdrawal of Cup/Rap

To determine changes in hippocampal neurogenesis in the demyelinated and remyelinated hippocampus, we first treated mice

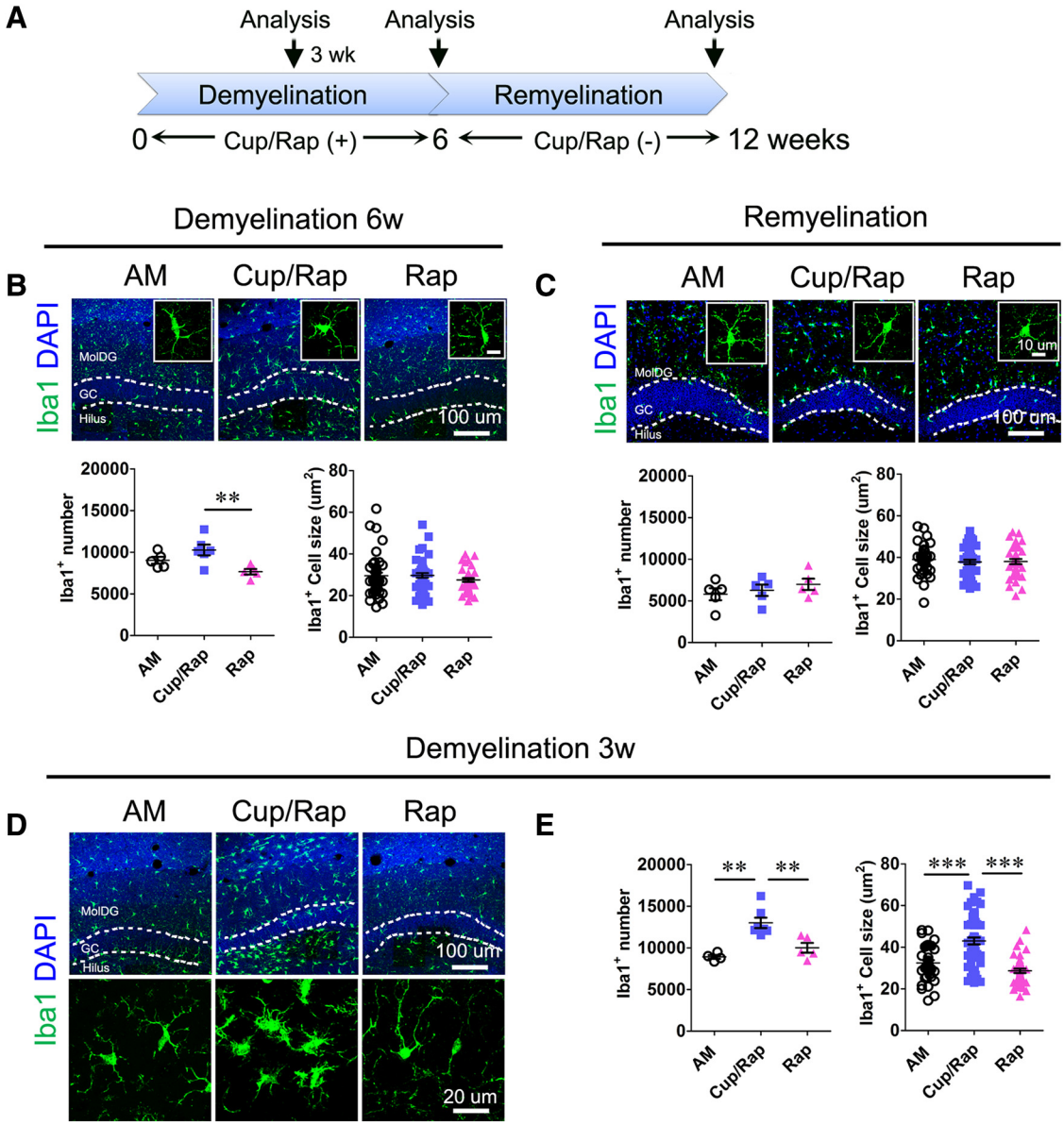

Figure 2. Early activation of microglia in dentate gyrus during demyelination. ***A***, Timeline of the experimental protocol. ***B***, Top, Representative images of Iba1 staining at 6 weeks of demyelination. Bottom, Quantification of microglia cell number and cell size. ***C***, Top, Representative images of Iba1 staining during remyelination. Bottom, Quantification of microglia cell number and cell size. ***D***, Representative images of Iba1 staining at 3 weeks of demyelination. ***E***, Quantification indicates significantly increased cell number and cell size of microglia at 3 weeks of demyelination. Demyelination: $n = 5$ for AM and Rap, 6 for Cup/Rap; remyelination: $n = 5$. For quantification of cell size, 40–50 cells were measured from 5–6 animals of each group. Data are expressed as mean ± SEM and analyzed by one-way ANOVA followed by Bonferroni's *post hoc* test. $^{**}p < 0.01$, $^{***}p < 0.001$.

with Cup/Rap to examine the proliferation index in the SGZ of the hippocampus, as well as in the SVZ of the lateral ventricles, which present two neurogenic niches (Fig. 4*A*). Treatment with both Cup/Rap and Cup alone significantly demyelinated the hippocampus and SVZ area compared with AM and Rap control groups (Fig. 4*B*,*C*; SGZ: $F_{(3,18)} = 37.79$, $p < 0.0001$, one-way ANOVA; SVZ: $F_{(3,18)} = 11.45$, $p = 0.0004$, one-way ANOVA). To determine proliferation index, BrdU was administered at the end of the 6 week treatment with Cup/Rap. Both SGZ and SVZ showed a reduced number of BrdU$^+$ cells in Cup/Rap mice, as well as in Cup mice (SGZ: $F_{(3,19)} = 93.41$, $p < 0.0001$, one-way ANOVA; SVZ: $F_{(3,19)} = 6.674$, $p = 0.0039$, one-way ANOVA), although the effects of Cup/Rap or Cup on proliferation were more severe in the SGZ as shown by the near absence of BrdU-incorporated cells (Fig. 4*D*,*E*). Consistent with reduced proliferation of NSCs in the SGZ, the DCX-immunopositive area was also abrogated in both Cup/Rap and Cup mice (Fig. 4*F*,*G*; $F_{(3,19)} = 83.76$, $p < 0.0001$, one-way ANOVA). Interestingly, the reduction in the coverage of DCX-immunopositive area was only evident in the SVZ of Cup/Rap mice ($F_{(3,19)} = 4.26$, $p = 0.0216$, one-way ANOVA), suggesting a differential sensitivity of proliferating cells in the SGZ and SVZ to treatment with Cup/Rap (Fig. 4*F*,*G*).

Interestingly, this decreased proliferation index reverted to control levels in the SGZ after 6 weeks of withdrawal from Cup/Rap. The numbers of Ki67$^+$ cells, as well as CldU-incorporated cells, returned to basal levels (Fig. 4*H*,*I*; for Ki67: $F_{(2,14)} = 2.045$, $p = 0.1721$, one-way ANOVA; for CldU: $F_{(2,14)} = 0.7260$, $p = 0.5039$, one-way ANOVA). Increased proliferation of NSCs normalized the production of newborn neurons, showing DCX expression that was indistinguishable from control mice in the remyelinated hippocampus (Fig. 4*H*,*I*; $F_{(2,14)} = 0.7252$, $p = 0.5043$, one-way ANOVA).

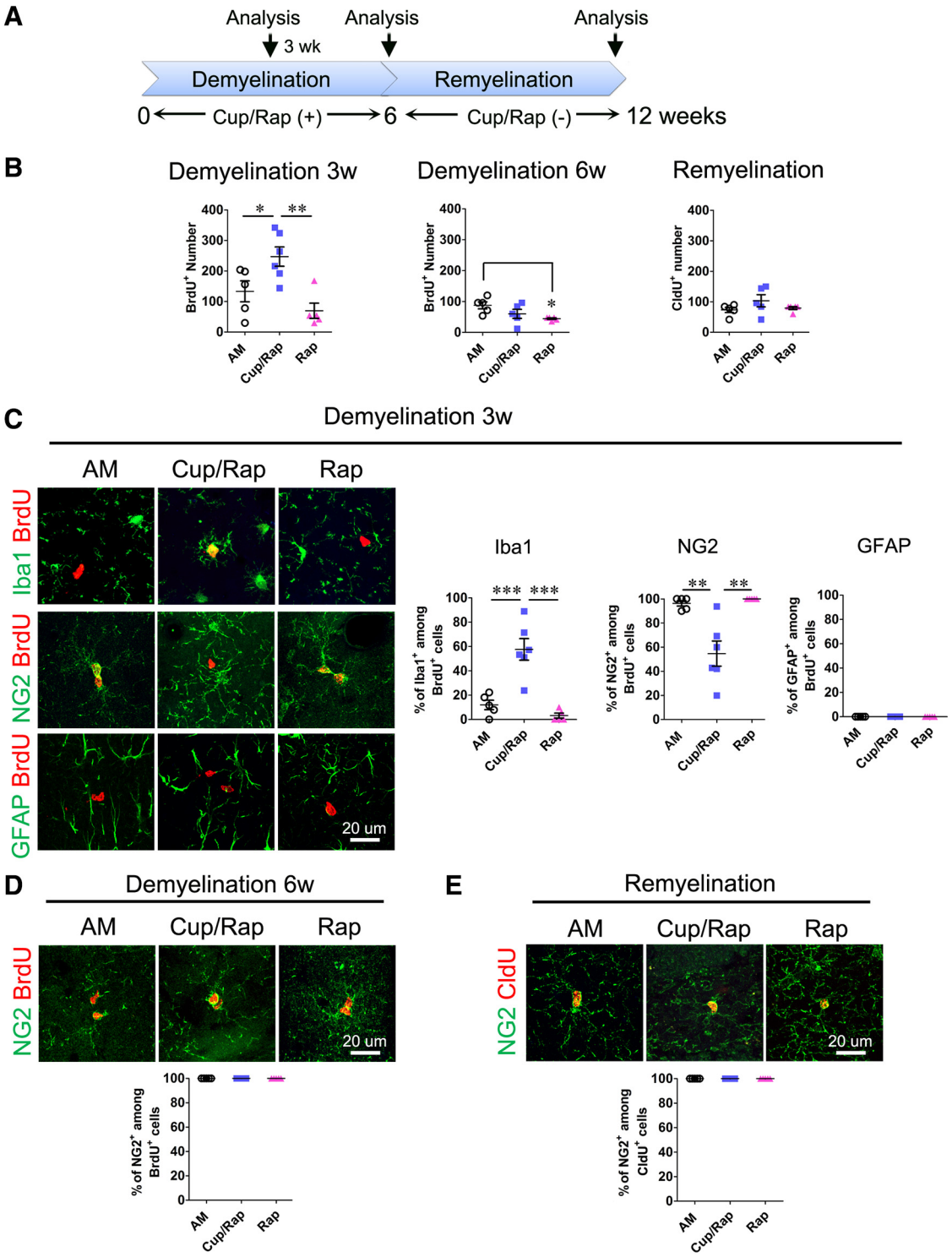

Figure 3. Proliferation of glial cells in the DG during demyelination and remyelination. ***A***, Timeline of the experimental protocol. ***B***, BrdU number at 3 weeks and 6 weeks of demyelination, and CldU number at 6 weeks of remyelination. BrdU number increases at 3 weeks of demyelination, but not at 6 weeks of demyelination or remyelination. ***C***, Representative images showing increased dividing microglia (colocalization of Iba1 and BrdU) and decreased colocalization of NG2 with BrdU in the Cup/Rap group at 3 weeks of demyelination. No colocalization of GFAP with BrdU was found at this time point. ***D***, Colocalization of NG2 with BrdU at 6 weeks of demyelination. The results indicate that all of the BrdU $^{+}$ cells are NG2 $^{+}$. ***E***, Colocalization of NG2 with CldU during remyelination. The results indicate that all of the CldU $^{+}$ cells are NG2 $^{+}$. Demyelination: $n = 5$ for AM and Rap, 6 for Cup/Rap; remyelination: $n = 5$. Data are expressed as mean ± SEM and analyzed by one-way ANOVA followed by Bonferroni's *post hoc* test. *$p < 0.05$, **$p < 0.01$, ***$p < 0.001$.

NSCs become proliferatively quiescent in the Cup/Rap-induced demyelinated hippocampus

To test whether the reduced number of NSCs is attributable to decreased proliferation in the demyelinated hippocampus, we quantified the density of NSCs in Cup/Rap mice. SOX2 and GFAP were used to identify and quantify radial glia (RG)-like NSCs or type 1 NSCs in the SGZ (Suh et al., 2009; Kempermann et al., 2015). The density of SOX2/GFAP double-positive type 1 NSCs did not change, indicating that the pool size of type 1 NSCs was maintained in Cup/Rap mice (Fig. 5*A–C*; $F_{(2,15)} = 0.2619$, one-way

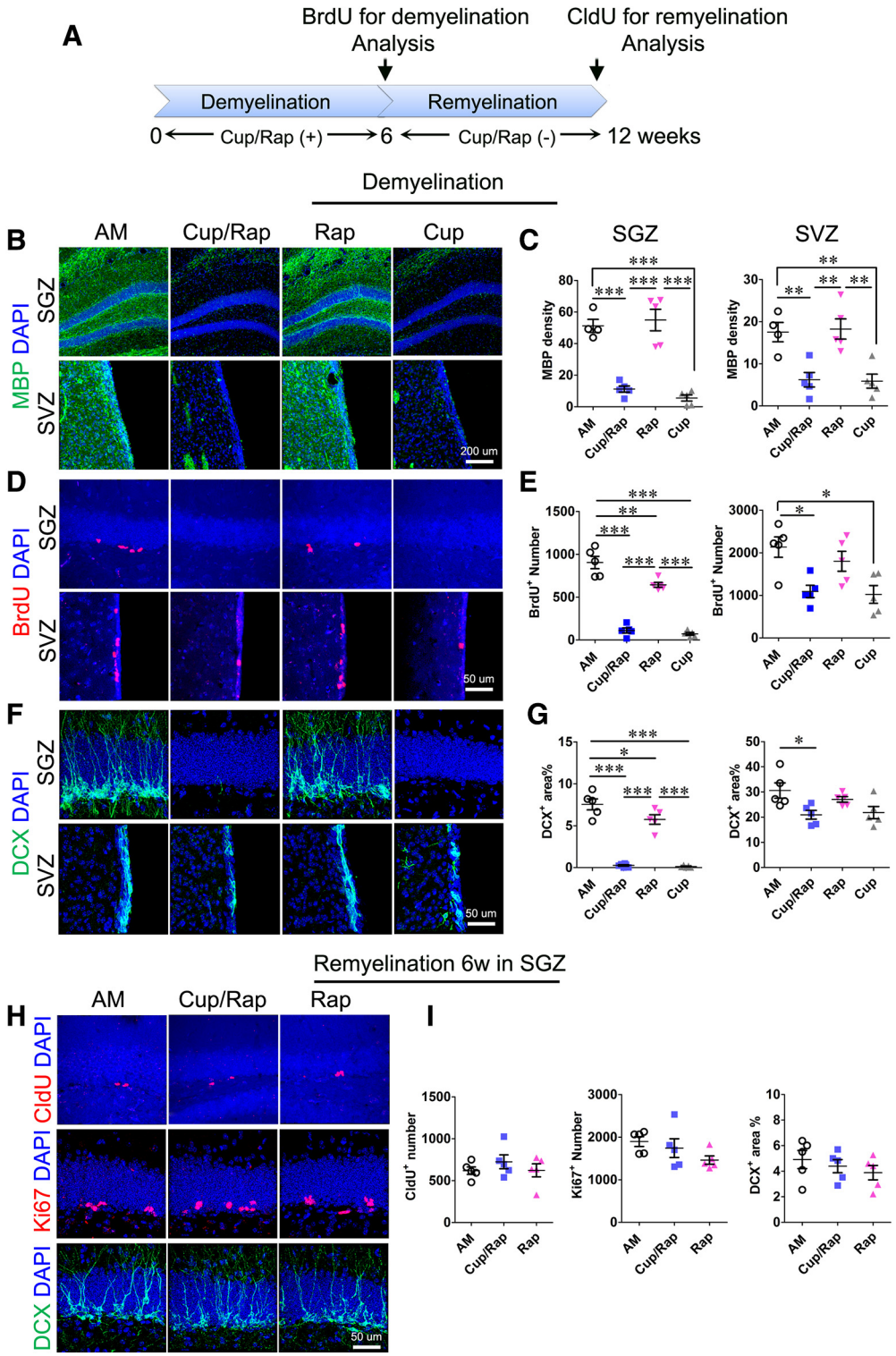

Figure 4. Neurogenesis is suppressed during demyelination and recovers during remyelination. ***A***, Timeline of the experimental protocol. ***B***, MBP staining of the SGZ and SVZ. ***C***, Quantification of MBP density indicates significantly reduced MBP expression in the SGZ and SVZ in Cup/Rap as well as Cup mice. ***D***, BrdU staining of SGZ and SVZ. ***E***, BrdU $^{+}$ cell number in SGZ and SVZ was significantly decreased in both the Cup/Rap and Cup groups. ***F***, DCX staining of SGZ and SVZ. ***G***, Percentage of DCX $^{+}$ coverage of the granular cell layer and SVZ. DCX coverage was significantly decreased in the SGZ in the Cup/Rap and Cup groups, and was significantly decreased in the SVZ in the Cup/Rap group. ***H***, CldU, Ki67, and DCX staining of the SGZ after 6 weeks of remyelination. ***I***, CldU $^{+}$, Ki67 $^{+}$ cell number and DCX coverage for SGZ. The quantification is comparable among groups during remyelination; $n = 5–6$. Data are expressed as mean ± SEM and analyzed by one-way ANOVA followed by Bonferroni's *post hoc* test. *$p < 0.05$, **$p < 0.01$, ***$p < 0.001$.

ANOVA). MCM2 is a G_1 phase-specific marker and has been used to determine the proliferation state of hippocampal NSCs (Maslov et al., 2004; Suh et al., 2007; Song et al., 2012). The number of MCM2 $^{+}$ cells was significantly decreased in Cup/Rap mice (Fig. 5*D*, *E*; $F_{(2,15)} = 36.17$, $p < 0.0001$, one-way ANOVA). More importantly, while 6.47 ± 0.87% of GFAP/SOX2 double-positive type 1 NSCs expressed MCM2 in AM control mice, none of the type 1 NSCs showed MCM2 expression in Cup/Rap mice,

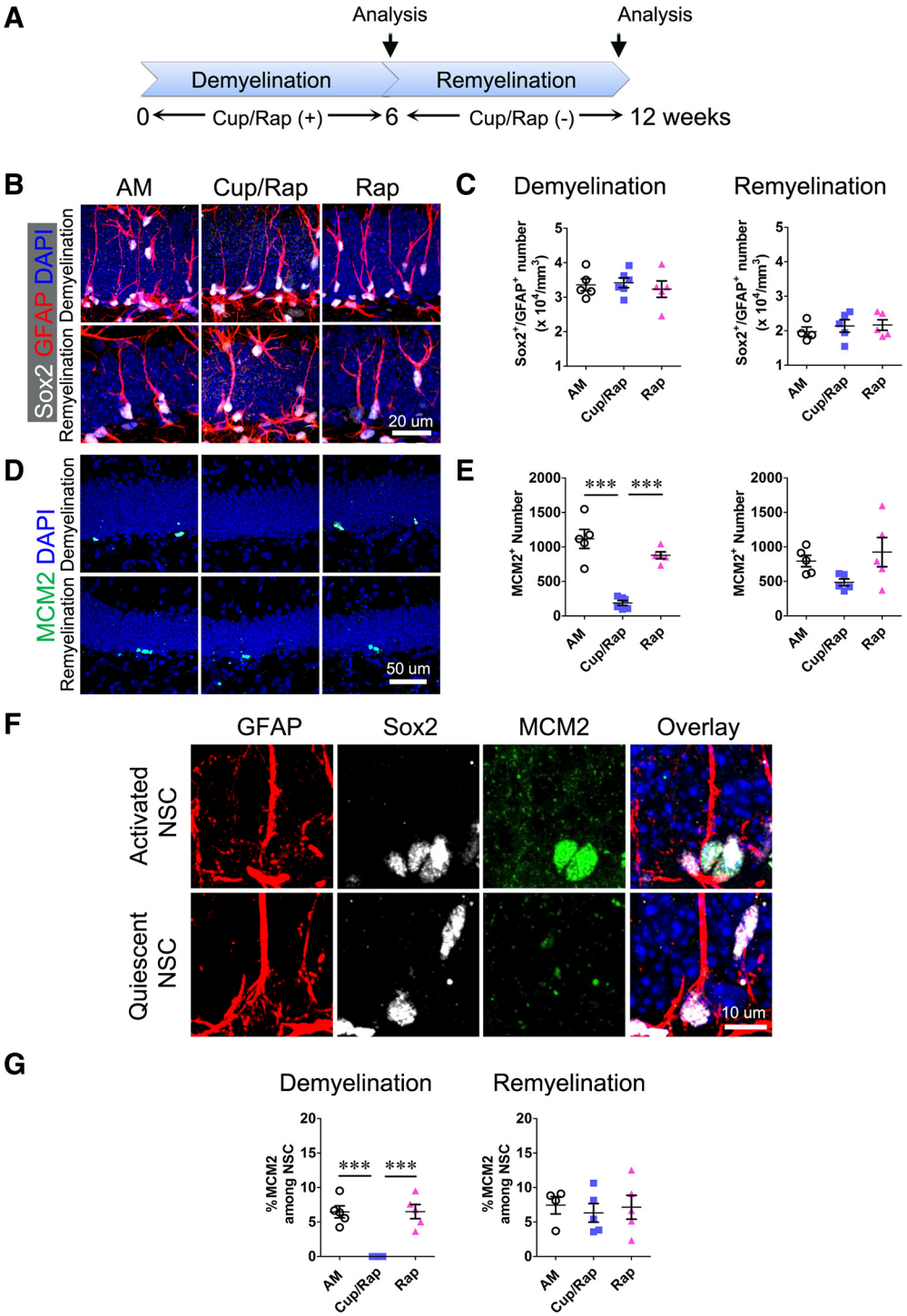

Figure 5. Demyelination does not alter NSC pool size, but inhibits proliferation of NSCs. ***A***, Timeline of the experimental protocol. ***B***, NSCs are identified as GFAP$^+$/Sox2$^+$ with radial morphology. ***C***, Quantification results indicate no significant effects of demyelination or remyelination on NSC number. ***D***, MCM2 staining of dentate gyrus. ***E***, Quantification of MCM2$^+$ cell number, which was significantly decreased following demyelination and recovered following remyelination. ***F***, Representative images showing activated (MCM2$^+$) NSCs and quiescent (MCM2$^-$) NSCs. ***G***, Percentage of activated NSCs assessed by percentage of MCM2$^+$ cell number among total NSCs. The quantification indicates that the percentage of activated NSCs was significantly decreased following demyelination and recovered following remyelination. Demyelination: $n = 5$ for AM and Rap, 6 for Cup/Rap; remyelination: $n = 5$. Data are expressed as mean ± SEM and analyzed by one-way ANOVA followed by Bonferroni's *post hoc* test. ***$p < 0.001$.

indicating that type 1 NSCs shifted to a proliferatively-quiescent state in Cup/Rap mice (Fig. 5*F*,*G*; $F_{(2,15)} = 23.32$, $p < 0.0001$, one-way ANOVA). Consistent with normalized proliferation in the SGZ during the withdrawal of Cup/Rap, the number of SOX2/GFAP double-positive type 1 NSCs ($F_{(2,14)} = 0.3928$, $p = 0.6843$, one-way ANOVA), MCM2$^+$ cells ($F_{(2,14)} = 2.819$, $p = 0.0992$, one-way ANOVA), as well as MCM2/GFAP/SOX2 triple-positive type 1 NSCs ($F_{(2,14)} = 0.1457$, $p = 0.8661$, one-way ANOVA) were restored to control levels (Fig. 5*B*–*G*) during a 6 week withdrawal of Cup/Rap.

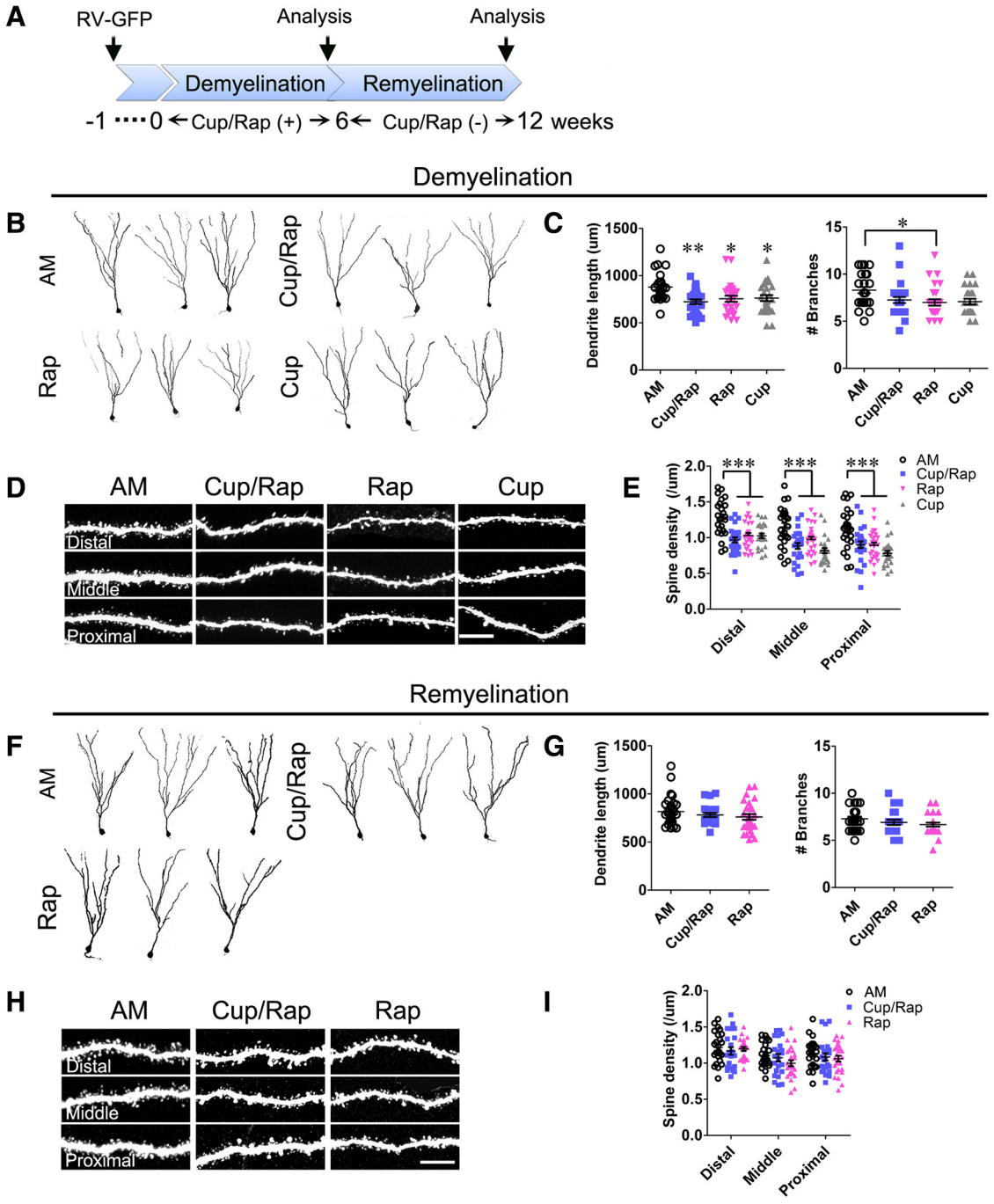

Figure 6. Dendritic morphology and spine density of hippocampal newborn neurons during demyelination and remyelination. ***A***, Timeline of the experimental protocol. ***B***, Representative images of hippocampal newborn neurons in demyelinated mice. ***C***, Measurements of dendritic length and number of branches. The results indicate a significant decrease in dendritic length in the Cup/Rap group, as well as in the Cup or Rap alone groups. ***D***, Representative images showing dendritic spines from distal, middle, and proximal segments of dendrite. ***E***, Quantification of spine density. The spine density is significantly reduced in the Cup/Rap group, and also in the Cup or Rap alone group. ***F***, Representative images of hippocampal newborn neurons in remyelinated mice. ***G***, Measurements of dendritic length and number of branches. ***H***, Representative images showing dendritic spines from distal, middle, and proximal segments of dendrite. ***I***, Quantification of spine density. The spine density is comparable among groups during remyelination. Twenty-two to 30 GFP-labeled newborns from five animals per group were analyzed. Scale bar, 10 μm. Data are expressed as mean ± SEM and analyzed by one-way ANOVA followed by Bonferroni's *post hoc* test. *$p < 0.05$, **$p < 0.01$, ***$p < 0.001$.

Dendritic length and spine density of newborn neurons are decreased in Cup/Rap mice

To investigate the development of hippocampal newborn DGCs in the demyelinated brain, we injected GFP-expressing retrovirus into the DG and examined the structure of newborn neurons during treatment and withdrawal of Cup/Rap (Fig. 6*A*). The total dendritic length of newborn neurons was decreased in Cup/Rap, Cup, and Rap mice compared with AM mice, whereas the number of dendritic branches was not affected in Cup/Rap or Cup mice (Fig. 6*B*,*C*; for length: $F_{(3,104)} = 5.411$, $p = 0.0017$, one-way ANOVA; for branch number: $F_{(3,104)} = 3.446$, $p = 0.0196$, one-way ANOVA). To determine synaptic connectivity of newborn DGCs with excitatory afferent neurons, we examined spine density in the distal, middle, and proximal segments of dendrites of hippocampal newborn DGCs. Spine density was globally decreased along the entire dendrite of newborn DGCs in Cup/Rap,

Cup, and Rap mice compared with AM mice (Fig. 6*D*,*E*; distal: $F_{(3,101)} = 11.89$, $p < 0.0001$; middle: $F_{(3,101)} = 10.48$, $p < 0.0001$; proximal: $F_{(3,101)} = 9.85$, $p < 0.0001$, one-way ANOVA). Interestingly, the total dendritic length and spine density of hippocampal newborn DGCs were restored during 6 weeks of withdrawal from Cup/Rap (Fig. 6*F–I*; for length: $F_{(2,79)} = 1.19$, $p = 0.3097$; distal density: $F_{(2,71)} = 0.3405$, $p = 0.7126$; middle density: $F_{(2,71)} = 1.83$, $p = 0.1681$; proximal density: $F_{(2,71)} = 0.7125$, $p = 0.4941$, one-way ANOVA), suggesting that the changes in structural development and synaptic connectivity of DGCs were reversibly normalized during the 6 week withdrawal period.

Discussion

MS is a neuroinflammatory disorder characterized by demyelination in CNS white matter, as well as the cortex and deep gray matter (Trapp and Nave, 2008). Demyelination disrupts axonal transmission, leading to deficits in sensory and motor functions. MS usually begins with reversible episodes of neurological disabilities and recovery, and ~85% of MS patients begin with this relapsing-remitting disease course; unfortunately, however, the majority of MS patients develop irreversible chronic conditions during later progressive phases (Noseworthy et al., 2000; Hauser and Oksenberg, 2006; Trapp and Nave, 2008). In addition to sensory and motor dysfunctions, cognitive impairments are significant comorbidities in MS. Indeed, up to 70% of MS patients suffer from various cognitive deficits in attention, information processing, execution, and long-term memory. Although cognitive impairments represent a serious health toll that negatively impacts the quality of life (Rao et al., 1991; Chiaravalloti and DeLuca, 2008), little is known about changes in the brain that link MS pathology to altered learning and memory in patients. In this study, using a Cup/Rap-induced MS mouse model (Bai et al., 2016), we investigated hippocampal neurogenesis as a surrogate to measure alterations of cognitive function in MS. Our study revealed that neurogenesis and synaptic connectivity of newborn neurons were impaired in the Cup/Rap-treated hippocampus. Interestingly, these alterations in neurogenesis and anatomical development of newborn neurons were normalized following withdrawal of Cup/Rap and subsequent remyelination. Thus, our study provides critical insight into reversible hippocampal neurogenesis, which can be used to intervene in and/or treat cognitive impairments associated with MS.

In this study, to understand neural substrates that may translate MS pathology into cognitive deficits, we investigated hippocampal neurogenesis in the Cup/Rap-induced demyelinated hippocampus. Hippocampal neurogenesis is a multistep process: each step of proliferation of NSCs, as well as survival and circuitry integration of newborn neurons, is critical to maintain homeostatic neurogenesis, and this tightly regulated process of neurogenesis is critical for cognition and emotion (Suh et al., 2009; Christian et al., 2014). Consequently, disruption of any of these steps in hippocampal neurogenesis results in cognitive impairments (Aimone et al., 2014). Among heterogeneous NSC populations that differ in proliferation kinetics, differentiation potential, morphology, and marker expression, RG or type 1 NSCs have been placed at the top of the NSC hierarchy because they represent NSCs that have the ability to self-renew and are multipotent (Suh et al., 2009; Christian et al., 2014; Kempermann et al., 2015). Therefore, the activity of type 1 NSCs is critical to maintain a quantitative balance between newborn cells and pre-existing cells in the hippocampus. We examined the role of type 1 NSCs in the reversible changes to neurogenesis in the demyelinated and remyelinated hippocampus induced by the treatment and withdrawal of Cup/Rap, respectively. First, SOX2 and GFAP double-immunohistochemistry showed that the number of type 1 NSCs remained unchanged in Cup/Rap mice. Next, we assessed the proliferation state of type 1 NSCs using MCM2, which is a marker for the G_1 phase of the cell cycle (Song et al., 2012, 2016). This approach revealed that the number of mitotically-quiescent type 1 NSCs (MCM2-negative population among $SOX2^+/GFAP^+$ cells) was significantly increased concomitant with a reduction in proliferatively-active type 1 NSCs ($MCM2^+/SOX2^+/GFAP^+$ cells) in Cup/Rap mice. Interestingly, the number of proliferatively-active type 1 NSCs returned to basal levels during withdrawal of Cup/Rap. Thus, our study revealed that a shift between proliferatively-active and mitotically-quiescent states of type 1 NSCs is tightly associated with acute demyelination and following remyelination in Cup/Rap mice, whereas the size of the NSC reservoir remained unchanged. As shown in a previous report that increasing the number of hippocampal newborn neurons was sufficient to counteract impaired hippocampal function such as depression (Sahay et al., 2011), maintenance of the NSC reservoir and the reversible nature of neurogenesis raise an important possibility that hippocampal neurogenesis can be reactivated to intervene in cognitive impairments associated with MS (Plemel et al., 2017).

In addition to the level of neurogenesis, the structural development of newborn neurons was also impaired in Cup/Rap mice. Taking advantage of a birth-date labeling method that uses a GFP-expression retrovirus (Golub et al., 2015), we labeled newborn neurons in an age-synchronized manner and examined the development of gross morphology and dendritic spines of hippocampal newborn DGCs. Although the total dendritic lengths and spine density were significantly reduced in Cup/Rap mice, both were also normalized during withdrawal of Cup/Rap. These results are consistent with a previous report showing synaptic alterations in the hippocampus of MS patients (Dutta et al., 2011). Excitatory neurons located in the lateral and medial entorhinal cortex, as well as in the hilus, project to and form spines in the outer, middle, and inner segments of dendrites of newborn neurons in a topological manner (Amaral et al., 2007). Therefore, dendritic spine density, as well as relative positions of spines along the dendrites, provide critical information on synaptic connectivity as well as the origin of presynaptic partners. Our analysis showed reduced spine density throughout the dendrites of newborn neurons, indicating a global reduction in synaptic connectivity between hippocampal newborn DGCs and excitatory neurons such as entorhinal neurons and hilar mossy cells, further supporting the concept that decreased synaptic connectivity with afferent input neurons impairs information flow and processing, and thereby cognitive function, in MS patients.

Interestingly, the decreased neurogenesis and synaptic connectivity of hippocampal DGCs returned to basal levels in the remyelinated hippocampus. These results raise an important possibility that key neural structures necessary for cognitive function remain intact in the demyelinated hippocampus and that these components can be reactivated to treat MS. Indeed, in our MS mouse model in which withdrawal of Cup/Rap induced remyelination, the expression of myelin proteins such as PLP and MBP recovered to normal levels and the number of mature oligodendrocytes also recovered. Concomitant with remyelination in the hippocampus, the proliferation index, as well as synaptic connectivity, accelerated and reached levels comparable to those in control mice. Unlike many neurodegeneration models in which hippocampal NSCs are dead and hippocampal neurogenesis is permanently damaged as a consequence, our study raises the possibility that the NSC reservoir might be preserved in the demyeli-

nated hippocampus, but the production of new cells may be temporarily halted by shifting NSCs from a mitotically-active state to a proliferatively-dormant state. In the remyelinated hippocampus, NSCs became mitotically active and neurogenesis was reinitiated. This reversible nature of neurogenesis during demyelination and remyelination raises an important implication in therapeutic application to treat and cure cognitive impairments in MS patients by directly manipulating hippocampal neurogenesis (Plemel et al., 2017; Kremer et al., 2019).

The precise mechanism that links demyelination to reduced neurogenesis and synaptic connectivity is speculative. First, reduced brain activity caused by demyelination may negatively impact hippocampal neurogenesis and synapse formation. This is possible because brain activity is a critical regulator for both proliferation and synaptic connectivity (Song et al., 2016; Donato et al., 2017). For example, chemical stimulation or induction of long-term potentiation followed by electrical stimulation of the perforant pathway increased proliferation and spine formation in the hippocampus (Bruel-Jungerman et al., 2006; Danzer, 2012; Bromer et al., 2018). Excitatory neurons located in the entorhinal cortex (EC) project axons to and make direct synaptic connections with hippocampal DGCs (Zhou et al., 2019). EC-DG neural circuits play a key role in spatial and contextual memory. Therefore, it is plausible that demyelination of entorhinal neurons may reduce activity in the hippocampus, and this decreased neuronal activity, in turn, reduces neurogenesis and synaptic connections (Song et al., 2016; Monje, 2018). The second possibility is that demyelination indirectly influences neurogenesis and synaptic connections via inflammation (Monje et al., 2003; Sierra et al., 2010). In response to demyelination, it has been shown that microglia are activated and secrete inflammatory cytokines and/or chemokines, which may negatively regulate hippocampal neurogenesis and synapse formation (Abe et al., 2015). Indeed, our results showed that the number and size of microglia were significantly increased in the hippocampus during early stages of demyelination. Thus, the inflammatory response via activated microglia may indirectly decrease neurogenesis and synaptic connectivity during demyelination. Alternatively, cuprizone may have a direct effect on proliferation of type 1 NSCs and synaptic connectivity in addition to its toxicity to mature oligodendrocytes. To test this possibility, we examined the proliferation capacity of NSCs in 1 mM cuprizone, a minimal concentration that kills mature oligodendrocytes, in M03.13 cells *in vitro* (Bénardais et al., 2013). In this experiment, we observed that cultured hippocampal NSCs proliferated at a dramatically reduced rate in the presence of 1 mM cuprizone (data not shown). Although this result may imply a negative effect of cuprizone on proliferation of NSCs, further research is necessary to confirm that the active concentration of cuprizone could reach such a high level in the hippocampus and to rule out the involvement of indirect biological effects induced by demyelination such as inflammation in proliferation of NSCs and synaptic connectivity. Recognizing the complexity of rodent models of MS, our studies identify hippocampal neurogenesis as possible target for therapeutic intervention in individuals with MS.

References

Abe H, Tanaka T, Kimura M, Mizukami S, Saito F, Imatanaka N, Akahori Y, Yoshida T, Shibutani M (2015) Cuprizone decreases intermediate and late-stage progenitor cells in hippocampal neurogenesis of rats in a framework of 28-day oral dose toxicity study. Toxicol Appl Pharmacol 287:210–221.

Acs P, Kipp M, Norkute A, Johann S, Clarner T, Braun A, Berente Z, Komoly S, Beyer C (2009) 17beta-estradiol and progesterone prevent cuprizone provoked demyelination of corpus callosum in male mice. Glia 57:807–814.

Aimone JB, Li Y, Lee SW, Clemenson GD, Deng W, Gage FH (2014) Regulation and function of adult neurogenesis: from genes to cognition. Physiol Rev 94:991–1026.

Amaral DG, Scharfman HE, Lavenex P (2007) The dentate gyrus: fundamental neuroanatomical organization (dentate gyrus for dummies). Prog Brain Res 163:3–22.

Bai CB, Sun S, Roholt A, Benson E, Edberg D, Medicetty S, Dutta R, Kidd G, Macklin WB, Trapp B (2016) A mouse model for testing remyelinating therapies. Exp Neurol 283:330–340.

Bénardais K, Kotsiari A, Skuljec J, Koutsoudaki PN, Gudi V, Singh V, Vulinović F, Skripuletz T, Stangel M (2013) Cuprizone [bis(cyclohexylidenehydrazide)] is selectively toxic for mature oligodendrocytes. Neurotox Res 24:244–250.

Bromer C, Bartol TM, Bowden JB, Hubbard DD, Hanka DC, Gonzalez PV, Kuwajima M, Mendenhall JM, Parker PH, Abraham WC, Sejnowski TJ, Harris KM (2018) Long-term potentiation expands information content of hippocampal dentate gyrus synapses. Proc Natl Acad Sci U S A 115:E2410–E2418.

Bruel-Jungerman E, Davis S, Rampon C, Laroche S (2006) Long-term potentiation enhances neurogenesis in the adult dentate gyrus. J Neurosci 26:5888–5893.

Chiaravalloti ND, DeLuca J (2008) Cognitive impairment in multiple sclerosis. Lancet Neurol 7:1139–1151.

Christian KM, Song H, Ming GL (2014) Functions and dysfunctions of adult hippocampal neurogenesis. Annu Rev Neurosci 37:243–262.

Danzer SC (2012) Depression, stress, epilepsy and adult neurogenesis. Exp Neurol 233:22–32.

Donato F, Jacobsen RI, Moser MB, Moser EI (2017) Stellate cells drive maturation of the entorhinal-hippocampal circuit. Science 355:eaai8178.

Dutta R, Chang A, Doud MK, Kidd GJ, Ribaudo MV, Young EA, Fox RJ, Staugaitis SM, Trapp BD (2011) Demyelination causes synaptic alterations in hippocampi from multiple sclerosis patients. Ann Neurol 69:445–454.

Dutta R, Chomyk AM, Chang A, Ribaudo MV, Deckard SA, Doud MK, Edberg DD, Bai B, Li M, Baranzini SE, Fox RJ, Staugaitis SM, Macklin WB, Trapp BD (2013) Hippocampal demyelination and memory dysfunction are associated with increased levels of the neuronal microRNA miR-124 and reduced AMPA receptors. Ann Neurol 73:637–645.

Gage FH (2002) Neurogenesis in the adult brain. J Neurosci 22:612–613.

Gilmore CP, Donaldson I, Bö L, Owens T, Lowe J, Evangelou N (2009) Regional variations in the extent and pattern of grey matter demyelination in multiple sclerosis: a comparison between the cerebral cortex, cerebellar cortex, deep grey matter nuclei and the spinal cord. J Neurol Neurosurg Psychiatry 80:182–187.

Golub HM, Zhou QG, Zucker H, McMullen MR, Kokiko-Cochran ON, Ro EJ, Nagy LE, Suh H (2015) Chronic alcohol exposure is associated with decreased neurogenesis, aberrant integration of newborn neurons, and cognitive dysfunction in female mice. Alcohol Clin Exp Res 39:1967–1977.

Hauser SL, Oksenberg JR (2006) The neurobiology of multiple sclerosis: genes, inflammation, and neurodegeneration. Neuron 52:61–76.

Kempermann G, Song H, Gage FH (2015) Neurogenesis in the adult hippocampus. Cold Spring Harb Perspect Biol 7:a018812.

Kremer D, Akkermann R, Küry P, Dutta R (2019) Current advancements in promoting remyelination in multiple sclerosis. Mult Scler 25:7–14.

Longoni G, Rocca MA, Pagani E, Riccitelli GC, Colombo B, Rodegher M, Falini A, Comi G, Filippi M (2015) Deficits in memory and visuospatial learning correlate with regional hippocampal atrophy in MS. Brain Struct Funct 220:435–444.

Maslov AY, Barone TA, Plunkett RJ, Pruitt SC (2004) Neural stem cell detection, characterization, and age-related changes in the subventricular zone of mice. J Neurosci 24:1726–1733.

Monje M (2018) Myelin plasticity and nervous system function. Annu Rev Neurosci 41:61–76.

Monje ML, Toda H, Palmer TD (2003) Inflammatory blockade restores adult hippocampal neurogenesis. Science 302:1760–1765.

Noseworthy JH, Lucchinetti C, Rodriguez M, Weinshenker BG (2000) Multiple sclerosis. N Engl J Med 343:938–952.

Papadopoulos D, Dukes S, Patel R, Nicholas R, Vora A, Reynolds R (2009)

Substantial archaeocortical atrophy and neuronal loss in multiple sclerosis. Brain Pathol 19:238–253.

Plemel JR, Liu WQ, Yong VW (2017) Remyelination therapies: a new direction and challenge in multiple sclerosis. Nat Rev Drug Discov 16:617–634.

Preziosa P, Rocca MA, Pagani E, Stromillo ML, Enzinger C, Gallo A, Hulst HE, Atzori M, Pareto D, Riccitelli GC, Copetti M, De Stefano N, Fazekas F, Bisecco A, Barkhof F, Yousry TA, Arévalo MJ, Filippi M (2016) Structural MRI correlates of cognitive impairment in patients with multiple sclerosis. Hum Brain Mapp 37:1627–1644.

Rao SM, Leo GJ, Bernardin L, Unverzagt F (1991) Cognitive dysfunction in multiple sclerosis. I. frequency, patterns, and prediction. Neurology 41:685–691.

Sachs HH, Bercury KK, Popescu DC, Narayanan SP, Macklin WB (2014) A new model of cuprizone-mediated demyelination/remyelination. ASN Neuro 6:1–16.

Sahay A, Scobie KN, Hill AS, O'Carroll CM, Kheirbek MA, Burghardt NS, Fenton AA, Dranovsky A, Hen R (2011) Increasing adult hippocampal neurogenesis is sufficient to improve pattern separation. Nature 472:466–470.

Sierra A, Encinas JM, Deudero JJ, Chancey JH, Enikolopov G, Overstreet-Wadiche LS, Tsirka SE, Maletic-Savatic M (2010) Microglia shape adult hippocampal neurogenesis through apoptosis-coupled phagocytosis. Cell Stem Cell 7:483–495.

Song J, Zhong C, Bonaguidi MA, Sun GJ, Hsu D, Gu Y, Meletis K, Huang ZJ, Ge S, Enikolopov G, Deisseroth K, Luscher B, Christian KM, Ming GL, Song H (2012) Neuronal circuitry mechanism regulating adult quiescent neural stem-cell fate decision. Nature 489:150–154.

Song J, Olsen RH, Sun J, Ming GL, Song H (2016) Neuronal circuitry mechanisms regulating adult mammalian neurogenesis. Cold Spring Harb Perspect Biol 8:a018937.

Suh H, Consiglio A, Ray J, Sawai T, D'Amour KA, Gage FH (2007) *In vivo* fate analysis reveals the multipotent and self-renewal capacities of Sox2+ neural stem cells in the adult hippocampus. Cell Stem Cell 1:515–528.

Suh H, Deng W, Gage FH (2009) Signaling in adult neurogenesis. Annu Rev Cell Dev Biol 25:253–275.

Taylor LC, Gilmore W, Matsushima GK (2009) SJL mice exposed to cuprizone intoxication reveal strain and gender pattern differences in demyelination. Brain Pathol 19:467–479.

Trapp BD, Nave KA (2008) Multiple sclerosis: an immune or neurodegenerative disorder? Annu Rev Neurosci 31:247–269.

Trapp BD, Vignos M, Dudman J, Chang A, Fisher E, Staugaitis SM, Battapady H, Mork S, Ontaneda D, Jones SE, Fox RJ, Chen J, Nakamura K, Rudick RA (2018) Cortical neuronal densities and cerebral white matter demyelination in multiple sclerosis: a retrospective study. Lancet Neurol 17:870–884.

Wallin MT, Culpepper WJ, Campbell JD, Nelson LM, Langer-Gould A, Marrie RA, Cutter GR, Kaye WE, Wagner L, Tremlett H, Buka SL, Dilokthornsakul P, Topol B, Chen LH, LaRocca NG; US Multiple Sclerosis Prevalence Workgroup (2019) The prevalence of MS in the united states: a population-based estimate using health claims data. Neurology 92:e1029–e1040.

Zhou QG, Nemes AD, Lee D, Ro EJ, Zhang J, Nowacki AS, Dymecki SM, Najm IM, Suh H (2019) Chemogenetic silencing of hippocampal neurons suppresses epileptic neural circuits. J Clin Invest 129:310–323.